Equivalent Circuit Modeling of a Rotary Piezoelectric Motor

El, Ghouti N.; Helbo, Jan

Publication date:
2000

Document Version
Også kaldet Forlagets PDF

EQUIVALENT CIRCUIT MODELING OF A ROTARY PIEZOELECTRIC MOTOR

N. ELGHOUTI
Institute of Electronic Systems,
Department of Control Engineering
Aalborg University
Fredrik Bajers Vej 7, DK-9220 Aalborg Ø,
Denmark
E-mail: nel@control.auc.dk

J. HELBO
Institute of Electronic Systems,
Department of Control Engineering
Aalborg University
Fredrik Bajers Vej 7, DK-9220 Aalborg Ø,
Denmark
E-mail: jan@control.auc.dk

Abstract

In this paper, an enhanced equivalent circuit model of a rotary traveling wave piezoelectric ultrasonic motor "shinsei type USR60" is derived. The modeling is performed on the basis of an empirical approach combined with the electrical network method and some simplification assumptions about the physical behavior of the real system. This paper highlights the importance of the electromechanical coupling factor, which is responsible for the electrical to mechanical energy conversion. The emphasis is put on the difference between the effective coupling factor and the modal coupling factor. The effect of the temperature on the mechanical resonance frequency is considered and thereby integrated in the final model for long term operations.

keywords: Modeling, Piezoelectric Motor, Equivalent Circuit, Electromechanical Factor.

INTRODUCTION

The traveling wave Piezo Electric Motor (PEM) has excellent performance and many useful features such as high holding torque, high torque at low speed, quiet operation, simple structure, compactness in size and no electromagnetic interferences. However, the mathematical model of the PEM is complex and difficult to derive due to its driving principle based on high-frequency mechanical vibrations and frictional force [4]. Despite many attempts, a lumped motor model of the PEM is unavailable so far. The dynamical characteristics of the PEM are complicated, highly non-linear, and the parameters of the motor are time-varying due to temperature rise and changes in motor drive operating conditions. Therefore, it is difficult to predict the performance of the PEM under various working conditions.

Equivalent circuit modeling of the traveling wave UltraSonic Motor (USM) "shinsei type USR60" has been the subject of extensive research all over the world and important contributions have been established in [4]. In [3] a systematic modeling approach has been reported. The complexity of the conversion process of the the electromechanical energy within this device is daunting. The increase of temperature during operation affects the performance of the motor strongly. Despite many reported attempts, the modeling of this device is still a challenging problem. Therefore, an insight is needed in understanding how the electromechanical coupling factor, which guarantees the effective energy conversion, can be incorporated in the ECM in order for the simulated model to match better the performance of the physical system. It has been observed in practice that the mechanical resonance frequency of the motor shifts towards lower frequencies during the operation of the motor due to the temperature increase within the body of the stator. In order to overcome this problem a tracking facility which will update the temperature sensitive parameters is integrated in the equivalent circuit model presented in this paper.

This paper reports on the attempt to solve this highly demanding problem of performance prediction of the PEM. The rotary traveling wave ultrasonic motor "shinsei type USR60" is the case study considered in this paper. Consequently the objective is to derive a simple equivalent circuit model providing the ability to predict most of the motor performance under various working conditions.

BACKGROUND

For practical purposes it is sufficient to observe the electrical admittance of the PEM around its fundamental resonance frequency [1]. The admittance Y of any piezoelectric transducer is given by the sum of the damped Y_d

and the motional Y_m admittance

$$Y = Y_d + Y_m \tag{1}$$

Where

$$\begin{cases} Y_d = 1/R_d + j\omega C_d \\ Y_m = 1/[R + j(\omega L - 1/\omega C)]. \end{cases} \tag{2}$$

The identification of the admittance parameters (R_d, C_d, R, L, C) is carried out by using the electrical network method based on the Nyquist and the bode diagrams of the admittance [2].

The following figure 1 represents the locus of the admittance in Nyquist plane where the curve describes a vertical line with increasing frequency, except in the region around the mechanical resonance and antiresonance where it describes a motional admittance circle. The maximum and the minimum of the motional admittance occur at the mechanical resonance (series) f_s and antiresonance (parallel) f_p respectively. The resonance and the antiresonance of the whole system is given by f_r and f_a respectively whereas the maximum and the minimum of the total admittance are given by the pair f_h and f_l respectively. The admittance is capacitive over the whole range of frequencies except for the narrow diapason of frequencies lying between f_r and f_a where the admittance is inductive. The three pairs of characteristics frequencies (f_r,f_a) , (f_s,f_p) and (f_h,f_l) are therefore the frequencies of principal interest in the process of identification of the parameters of all two terminal equivalent circuit applications.

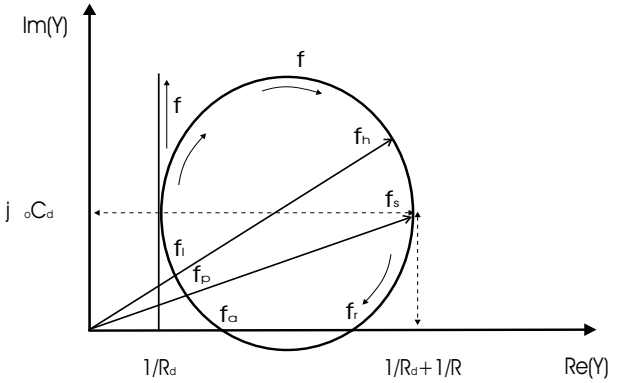

Figure 1: Nyquist diagram of the electromechanical transducer around its fundamental resonance and antiresonance frequencies

The electrical network method also uses the information provided by the frequency response as a Bode magnitude diagram where the three pairs of characteristic frequencies are identified in the neighborhood of the resonance and antiresonance sharpness of the diagram as shown in figure 2.

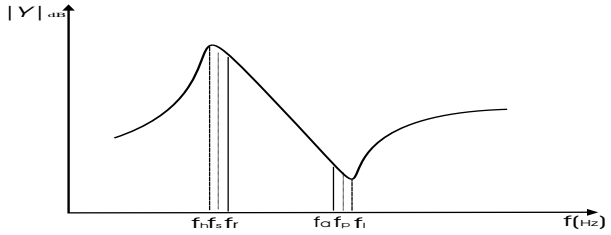

Figure 2: Bode magnitude diagram of the electromechanical transducer around its fundamental resonance and antiresonance frequencies

For convenience, definitions of characteristic parameters, obtained from the admittance diagram, are listed bellow

Motional (series) resonance frequency	$f_s = \frac{1}{2\pi\sqrt{LC}}$
Parallel resonance frequency	$f_p = \frac{\sqrt{(1+\frac{C_d}{C})}}{2\pi\sqrt{LC}}$
Resonance frequency f_r	$Re(Y) = 0$
Antiresonance frequency f_a	$Re(Y) = 0$
Frequency at maximum admittance	f_h
Frequency at minimum admittance	f_l
Mechanical quality factor	$Q = 2\pi f_s \frac{L}{R}$
Capacitance ratio	$\frac{C_d}{C} = \frac{f_s^2}{f_p^2 - f_s^2}$

The characteristic frequencies which are commonly used in the evaluation of the equivalent circuit parameters are f_s and f_p. It must be emphasized that when the quality factor is sufficiently high $(Q > 100)$ then the pair (f_s, f_p) is obtained from the average of the two other pairs

$$(f_s, f_p) = \frac{(f_h, f_l) + (f_r, f_a)}{2} \tag{3}$$

The quality factor Q is determined from either the Nyquist diagram or the Bode diagram. In the Bode case, the sharpness of the admittance around the resonance frequency as shown in the figure 3 is used to determine Q from the pass band at $-3dB$ of the frequency response

$$Q = \frac{f_s}{\Delta f_{-3dB}} \tag{4}$$

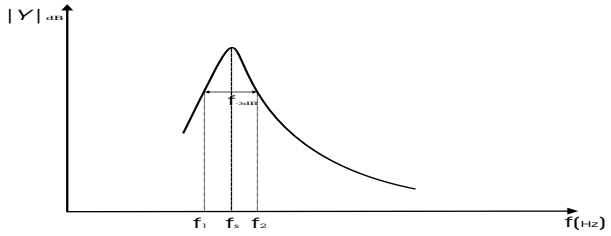

Figure 3: Bode magnitude diagram of the electromechanical transducer around its fundamental resonance frequency

From the Nyquist diagram the quality factor is

$$Q = 2\pi f_s \frac{L}{R} = \frac{1}{2\pi f_s RC} = \frac{1}{R}\sqrt{\frac{L}{C}} \tag{5}$$

Finally, the following set of equations gives the evaluation formula for each parameter in the two terminal equivalent circuit information

$$\begin{cases} f_s = \frac{f_h + f_r}{2} \\ f_p = \frac{f_l + f_a}{2} \\ R_d = \frac{1}{Re(Y(f))} \text{ for } f \ll f_s \\ C_d = \frac{Im(Y(f_s))}{2\pi f_s} \\ R = \frac{1}{Re(Y(f_s)) - \frac{1}{R_0}} \\ L = \frac{1}{4\pi^2 C_d (f_p^2 - f_s^2)} \\ C = C_d \frac{f_p^2 - f_s^2}{f_s^2} \\ Q = 2\pi f_s \frac{L}{R} > 100 \text{ for verification} \end{cases} \tag{6}$$

MODEL DERIVATION

The equivalent circuit modeling of the rotary PEM is done stepwise by first considering the free stator then the unloaded motor and finally the loaded motor.

THE FREE STATOR

The identification of the parameters of the equivalent circuit is carried out by applying the electrical network method as stated in the previous section. The stator of the PEM is a two phase symmetrical system with each phase providing a standing wave. Due to the special design of the stator these standing waves are combined and create a traveling wave within the body of the stator. The electrical admittance of each phase of the stator was measured in the same conditions and their compared results are plotted in the figure 4

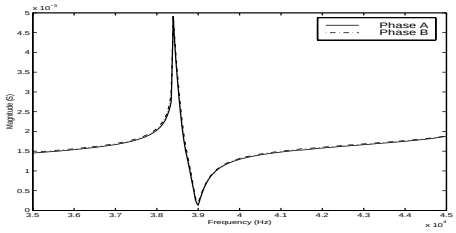

Figure 4: Comparison between the stator's two phase admittance around the fundamental resonance frequency

From the figure 4 it can be noticed that the two phases exhibit almost the same admittance, consequently the stator can be assumed to be perfectly symmetrical and therefore only one phase needs to be identified.

The admittance of the free stator is provided for one phase around the fundamental frequency, and the results are plotted in the figures 5 in the form of Bode magnitude and phase diagram.

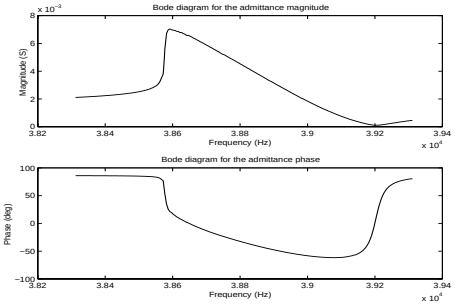

Figure 5: Bode magnitude and phase diagram of the electrical admittance of the stator around the fundamental resonance frequency

From the bode diagram it can easily be seen that the admittance exhibits resonance and antiresonance behavior in the explored range of frequencies. The extraction of the parameters is therefore possible by using the Nyquist diagram in the figure 6 according to the previously stated method.

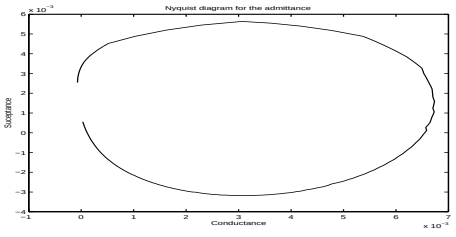

Figure 6: Nyquist diagram of the electrical admittance of the stator around the fundamental resonance frequency

The exploitation of the Nyquist diagram leads to the following values

fs =	3.862e+04	R =	149.75
fp =	3.920e+04	L =	0.102
R_d =	3.12e+04	C =	1.66e-10
C_d =	5.4e-09	Q =	166

The quality factor Q which is over 100 in this case enhances the validity of the approximation made to derive the parameters of the network.

The stator is by nature an electromechanical system with an electrical input terminal and a mechanical output terminal. The admittance of the stator derived in the above gave

the mechanical parameters of the network in terms of their electrical equivalents. It is possible and also more convenient to derive these parameters directly by measuring the ElectroMechanical (EM) admittance of the vibrating gain of the stator. The EM admittance is the ratio between the speed of the vibration at the surface of the stator and the input voltage. The EM motional admittance y_m as a function of the electromechanical output parameters (r,l,c) is then given by

$$y_m = 1/[r + j(\omega l - 1/\omega c)] \tag{7}$$

The electrical motional admittance and the electromechanical admittance are related by the electromechanical transformer Π such that

$$y_m = \frac{Y_m}{\Pi^2} \tag{8}$$

Consequently, the electromechanical parameters seen as their electrical equivalents becomes

$$R = \tfrac{r}{\Pi^2}\ ,\ L = \tfrac{l}{\Pi^2}\ ,\ C = \Pi^2 c \tag{9}$$

The figure 7 presents the Bode magnitude and the Nyquist diagrams of the EM admittance. The exploitation

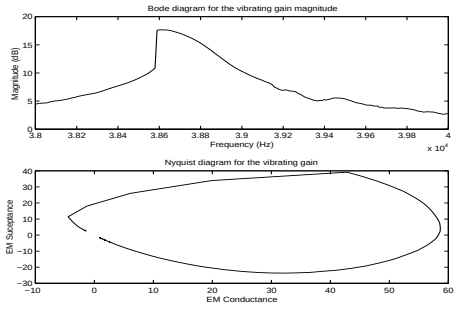

Figure 7: Bode and Nyquist diagram of the EM vibrating gain admittance of the stator around the fundamental resonance frequency

of the diagrams of the figure 7 according to the sharpness of the EM admittance around the resonance frequency, the derivation of the quality factor from the pass band at -3dB of the frequency response and considering the radius of the Nyquist diagram lead to the following values

fr =	3.8644e+04	r =	15.4
Δf_{-3dB} =	242.19	l =	0.0101
Q =	159.55	c =	1.68e-9

The quality factor which is slightly different from the previous case enhances both the validity of the approximation and the compatibility of these two methods. The above mechanical (r,l,c) values can be seen as their electrical equivalent and thereby deduce the force factor

$$\Pi = 0.32$$

The identified values are thereafter used in a simulated equivalent circuit model environment, and for each case an admittance is provided over a certain range of frequencies around the fundamental resonance and the results are then compared to the experimental data.

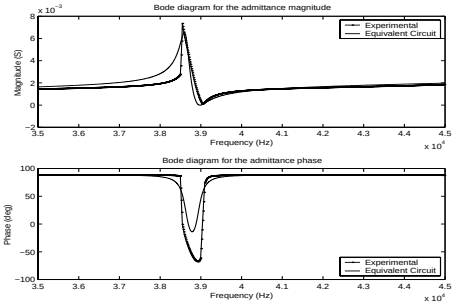

Figure 8: Prediction of the electrical admittance of the stator around the fundamental resonance frequency

From the figure 8 it can be noticed that the simulated model predicts most of the characteristic of the electrical admittance, especially in the range of frequencies located above the fundamental resonance. For control purposes the most important part of the equivalent circuit model is the mechanical output terminal. Therefore it is important to compare the EM admittance prediction to the experimental data.

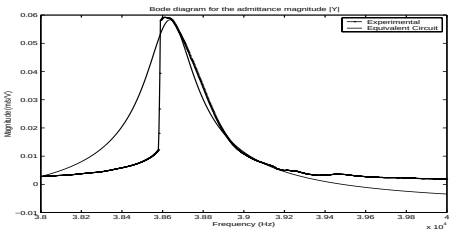

Figure 9: Prediction of the EM vibrating gain admittance of the stator around the fundamental resonance frequency

From the figure 9 it can be noticed that most of the characteristics of the vibrating gain can be predicted in a simulated environment. However, this is only valid in a narrow range of frequencies lying above the fundamental frequency.

THE MODAL FORCE FACTOR

The stator of USR60 is a two phase system in which a traveling wave is generated by the superposition of two standing waves provided by two excited mechanical orthogonal modes $\cos k\theta$ and $\sin k\theta$. The traveling wave can be mathematically expressed in terms of a summation over the excited mechanical modes weighted by their respective

modal amplitude ξ_1 and ξ_2 such that

$$\begin{cases} w(r,\theta,t) = R_r(\xi_1 \cos k\theta + \xi_2 \sin k\theta) \\ \qquad\qquad = R_r A \cos(\omega t - k\theta) \end{cases} \tag{10}$$

The speed of the traveling wave in normal direction (i.e. the rate of vibration) can be expressed by

$$\frac{dw}{dt} = -\vartheta \sin(\omega t - k\theta) = R_r(\dot{\xi}_1 \cos k\theta + \dot{\xi}_2 \sin k\theta) \tag{11}$$

where

$$\begin{cases} \xi_1 = A\cos\omega t \\ \xi_2 = A\sin\omega t \\ \vartheta = R_r A\omega \end{cases}$$

According to the piezoelectric converse effect the charge that flows in each electrode powering the electromechanical system is related to the generated displacement by a force factor. Therefore the modal amplitude of each excited mechanical mode is related by a modal force factor to the charge flowing into the motional part of the corresponding phase in the following way

$$\begin{cases} Q_{Am} = \eta\ \xi_1 \\ Q_{Bm} = \eta\ \xi_2 \end{cases} \tag{12}$$

which leads to the useful relation for the current and the modal amplitude velocity

$$\begin{cases} I_{Am} = \eta\ \dot{\xi}_1 \\ I_{Bm} = \eta\ \dot{\xi}_2 \end{cases} \tag{13}$$

Under the assumption that the two phases are symmetrical and powered by a common voltage the currents flowing in the motional part of the electromechanical system exhibits the same amplitude and therefore the following notation for the motional charge and current can be used

$$\begin{cases} Q_{Am} = Q_m \cos\omega t \\ Q_{Bm} = Q_m \sin\omega t \\ I_{Am} = -I_m \sin\omega t \\ I_{Bm} = I_m \cos\omega t \end{cases} \tag{14}$$

by rewriting the foregoing equation in terms of modal force factor and motional current the following is obtained

$$\begin{cases} w(r,\theta,t) = R_r(\frac{Q_m}{\eta}\cos\omega t\cos k\theta + \frac{Q_m}{\eta}\sin\omega t\sin k\theta) \\ \frac{dw}{dt} = \frac{R_r}{\eta}(-I_m\sin\omega t\cos k\theta + I_m\cos\omega t\sin k\theta) \\ \qquad = -R_r\frac{I_m}{\eta}\sin(\omega t - k\theta) \end{cases} \tag{15}$$

which leads to the following relation between the maximum of the vibration velocity and the maximum of the motional current flowing into each phase of the stator

$$\vartheta = R_r\frac{I_m}{\eta} \tag{16}$$

According to the force factor derived from the electromechanical parameters of the motional part seen as their electrical equivalents in the foregoing analysis the same relation is given by

$$\vartheta = \frac{I_m}{\Pi} \tag{17}$$

which leads to the following relation between the modal force factor and the overall force factor of the USR60

$$\eta = R_r\ \Pi \tag{18}$$

where R_r is a radial function depending on the design of the stator and the modal shape of the traveling wave in the radial direction. In general this function is given by the following relation

$$R_r = (\frac{r-a}{b-a})^\gamma \tag{19}$$

where a and b are the inner and outer radius of the annular plate of the stator respectively and γ is a constant depending on the modal shape of the deformation of the stator in the radial direction. By assuming that the contact interface between the stator and the rotor is mainly concentrated around the middle radius of the annular plate i.e. $R_m = \frac{b-a}{2}$ then R_r becomes a constant depending only on the amplitude of the radial mode at the point of contact. The choice of γ is however difficult but possible to derive from the motional part seen as its electrical equivalent powered by only one source of power leading to the same amplitude of vibration at the surface of the stator.

The total power needed to supply the two symmetrical phase USR60 is given by

$$P = V_A I_A + V_B I_B = 2VI \tag{20}$$

which can be written by

$$P = (\sqrt{2}V)(\sqrt{2}I) = V_c\ I_c \tag{21}$$

which suggests that if only one power source (i.e. one phase) is used to supply the stator of USR60 to obtain the same condition of vibration then the current that will flow in the motional part of the electromechanical system is given by

$$I_{cm} = \sqrt{2}\ I_m \tag{22}$$

The relation between the motional current and the vibration velocity is then given by

$$\vartheta = \frac{I_{cm}}{\Pi} = \frac{\sqrt{2}\ I_m}{\Pi} \tag{23}$$

The same amplitude of the vibration velocity could be achieved by the motional current I_m flowing through one phase of the stator by using the modal force factor η necessary to create a standing wave within the stator such that

$$\vartheta = \frac{I_m}{\eta} \tag{24}$$

which leads to

$$\Pi = \sqrt{2}\eta \tag{25}$$

and consequently

$$\begin{cases} \gamma = \frac{1}{2} \\ R_r = \frac{1}{\sqrt{2}} \end{cases} \tag{26}$$

THE UNLOADED MOTOR

The case of the unloaded motor with a rotor pressed against the stator with a normal forcing $F = 160\ N$ is the next step of the modeling process. Under the forcing process the piezoelectric converse effect tends to balance the external forcing when sufficient voltage is applied to the piezoceramic and therefore achieve the same resonance behavior (within the stator) around the fundamental resonance frequency. By assuming that the blocking admittance (R_d, C_d) characterizing the dielectric behavior of the stator remains constant under pressure and that the vibrating (modal) mass ℓ of the stator body is a mechanical constant then the only parameters subject to changes and therefore needing adjustments are (r, c) parameters of the mechanical terminal. Some extra resistance needs to be added in parallel with the blocking admittance at the terminal input in order to take into account the extra losses of power needed to overcome the external pressure and therefore meet the resonance of the stator.

MODELING THE APPLIED PRESSURE AND THE LOSSES

The extra losses due to pressure conditions can be integrated in the ECM as a power source P_f represented by a resistance R_f . For the USR60 these quantities can approximately be defined by the following relation [3].

$$\begin{cases} P_f = \frac{F}{80} \\ R_f = \frac{V^2}{P_f} \end{cases} \tag{27}$$

For the nominal condition of operation $F = 160\ N$ and $V = 100\ Vrms$ the loss of power is $P_f = 2\ W$ per phase which leads to a resistance $R_f = 5\ k\Omega$ to be integrated in parallel with the blocking admittance at the input terminal.

Besides the loss in power the frictional phenomenon at the stator and rotor contact points is responsible for more losses and also for performance deterioration in terms of speed drop. The frictional losses can be integrated in the model by readjusting the value of r at the mechanical terminal and readjusting the output speed of the model by substracting from the motional current at the output terminal a certain amount of current image of the speed drop seen as its electrical equivalent.

The readjustment of the mechanical resistance is done by simulation and by comparison to the experimental data gathered in terms of admittance of the unloaded motor operating in nominal conditions.

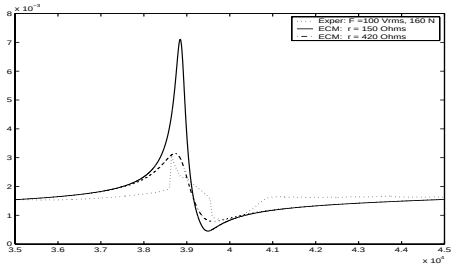

Figure 10: Readjustment of the mechanical damping by simulation in term of the admittance prediction of the rotary PEM

The figure 10 shows that the mechanical resistance seen as an electrical equivalent should be readjusted to $r = 420\ Ohms$ when the motor is operating under its nominal values $(100\ Vrms, 160\ N)$ in unloaded condition.

The speed drop can be provided by sensing the amplitude of the feedback voltage at different normal forcing with the excitation frequency maintained at its nominal value of 40 kHz . It is assumed that in ideal conditions the contact between the stator and the rotor is of a non sliding type and the velocity of the rotor is thereby opposite and equal to the maximum of the tangential velocity of the stator's particles which is given by

$$\vartheta = R_r A\omega = R_m \Omega_{id} \tag{28}$$

where A and ω are the amplitude and the angular frequency of the traveling wave at the surface of the stator, R_r is a mechanical constant depending only on the geometry of the stator, R_m is the middle radius of the driving contact and finally Ω_{id} is the rotary ideal speed of the motor's shaft. The figure 11 shows the speed-feedback characteristics at different normal loadings

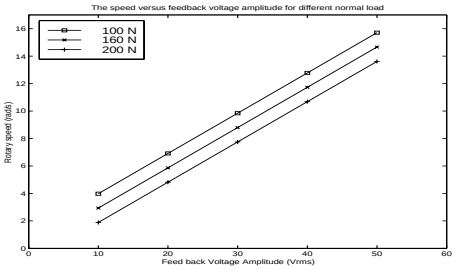

Figure 11: Speed-Feedback characteristics under different normal forcings

It is clear from the figure 11 that the speed of the unloaded motor depends on the normal forcing which is responsi-

ble for the sliding and the stick-slip behavior at the contact surface of the driving mechanism (friction). The measured speed Ω_o can be related to the ideal speed Ω_{id} by

$$\Omega_o = \Omega_{id} - \Delta\Omega_f \tag{29}$$

where $\Delta\Omega_f$ is the speed drop due to normal forcing. The above figure suggests that the speed drop is almost proportional to the normal forcing and their relationship is given by

$$\Delta\Omega_f \cong \alpha\ F \tag{30}$$

where for the USR60 the slop is $\alpha = 2\ 10^{-2}\ rad.s^{-1}.N^{-1}$.

The measured speed, drop speed and ideal speed can all be seen as their electrical equivalent and thereby be integrated in the equivalent circuit model of the unloaded motor. The speed relation leads to its current image relation for the current flowing in the motional impedance of the motor

$$\begin{cases} I_{m_o} = I_{id} - I_f \\ Arg(I_{m_o}) = Arg(I_{id}) = Arg(I_f) \end{cases} \tag{31}$$

Furthermore the speed current relationship obeys the following relation

$$\frac{\Omega_o}{I_{m_o}} = \frac{\Omega_{id}}{I_{id}} = \frac{\Delta\Omega_f}{I_f} = \aleph \tag{32}$$

The proportionality factor is easily derived from the ideal situation where the motional current is related to the tangential vibrating speed and the rotary speed by

$$I_{id} = \eta\vartheta = \eta R_m \Omega_{id} \tag{33}$$

which leads to

$$\aleph = \frac{1}{\eta R_m} \tag{34}$$

For the USR60 $R_m = 26.75$ mm, $\eta = 0.226$, the proportionality factor $\aleph = 165\ rad.s^{-1}.A^{-1}$ and $I_f = 19.4\ mA$.

Finally the rotary speed of the unloaded motor can be directly deduced from the motional current I_{m_o} by

$$\boxed{\begin{cases} \Omega_o = \aleph\ I_{m_o} & \text{for} \quad I_f \leqslant I_{m_o} \\ \Omega_o = 0 & \text{for} \quad I_f > I_{m_o} \end{cases}} \tag{35}$$

The equivalent circuit model of the unloaded motor can finally be represented by only a two terminal electrical network as shown in the figure 12 where all mechanical parameters are seen as their electrical equivalent.

It must be emphasised that the capacitance C_f in the two terminal equivalent circuit should be adjusted in order to mutch the mechanical resonance frequency of the unloaded motor under operation. The information on the mechanical resonance frequency is obtained by sensing the feedback signal.

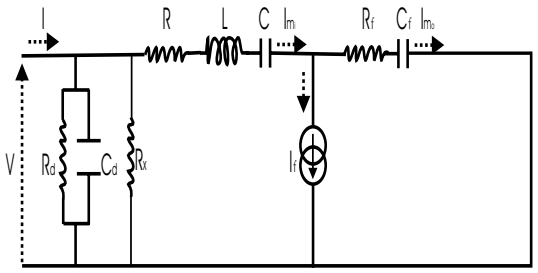

Figure 12: The ECM of the unloaded rotary PEM

THE LOADED MOTOR

The speed of the loaded motor depends on the amount of the torque load at the output shaft of the motor. The variational nature of the torque gives rise to nonlinear dynamical changes affecting the sliding and stick-slip behavior at the contact surface of the driving mechanism (friction). The measured speed Ω can be related to the ideal speed Ω_{id} by

$$\Omega = \Omega_{id} - \Delta\Omega_f - \Delta\Omega_\tau \tag{36}$$

where $\Delta\Omega_\tau$ is the speed drop due to the torque load. The following figures 13 and 14 shows that the speed drop is almost proportional to the torque load in the range of frequencies that are of interest i.e. $[40kHz, 41.5kHz]$

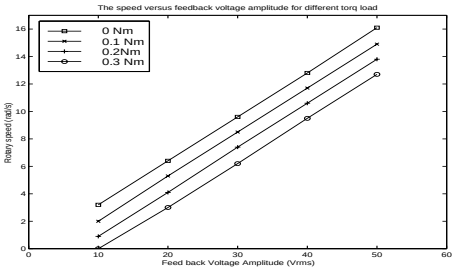

Figure 13: Speed-Feedback characteristics at different loading torque

The figures 13 and 14 suggest that the relationship between speed drop and torque load can be represented by the following linear equation where the coefficient β is the average slop of the speed-torque characteristics

$$\Delta\Omega_\tau \cong \beta\ T \tag{37}$$

where for the USR60 the slop is $\beta = 6.7\ rad.s^{-1}.N^{-1}.m^{-1}$.

The measured, drop and ideal speed can all be seen as their electrical equivalent and thereby be integrated in the equivalent circuit model of the unloaded motor. The speed relation leads to its current image relation for the current flowing in the motional impedance of the motor

$$\begin{cases} I_m = I_{id} - I_f - I_\tau \\ Arg(I_m) = Arg(I_{id}) = Arg(I_f) = Arg(I_\tau) \end{cases} \tag{38}$$

Furthermore the speed current relationship obeys the following relation

$$\frac{\Omega}{I_m} = \frac{\Omega_{id}}{I_{id}} = \frac{\Delta\Omega_f}{I_f} = \frac{\Delta\Omega_\tau}{I_\tau} = \aleph \tag{39}$$

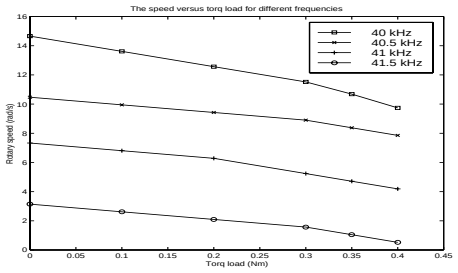

Figure 14: Speed-torque characteristics of the rotary PEM at different excitation frequencies

Finally the rotary speed of the loaded motor can be directly deduced from the motional current I_m by

$$\begin{cases} \Omega = \aleph\, I_m & \text{for} \quad I_f + I_\tau \leqslant I_m \\ \Omega = 0 & \text{for} \quad I_f + I_\tau > I_m \end{cases} \tag{40}$$

The proportionality factor is easily derived from the ideal situation as shown in the previous section and the equivalent circuit model of the loaded motor can finally be represented by a two terminal electrical network where all the mechanical parameters are seen as their electrical equivalents as shown in the figure 15

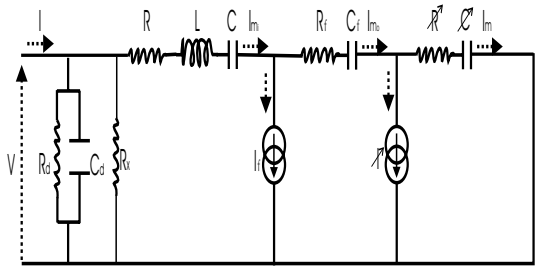

Figure 15: The ECM of the loaded rotary PEM

where the current I_τ image of the speed drop is torque dependant and given by

$$I_\tau = \frac{\beta}{\aleph} T \tag{41}$$

It must be emphasised that the (R_τ, C_τ) branch can be neglected in the simulation process.

TEMPERATURE INTEGRATION IN THE FINAL ECM

The resonance and antiresonance frequency changes with the temperature which in terms of equivalent circuit modeling can be represented by the same model as before but with varying parameters as shown in the figure 16

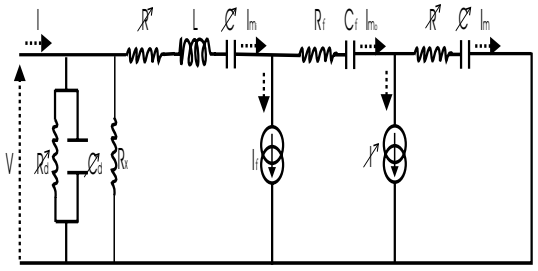

Figure 16: The complete ECM of the rotary PEM integrating the effect of temperature changes

The effect of the heating process that take place within the body of the stator on the performance of the PEM can be monitored by the feedback signal. The resonance frequency of the feedback signal shifts towards lower frequencies as the temperature of the PEM increase during the operation process. By sensing the feedback signal as a function of the temperature of the PEM the following characteristic shown in the figure 17 is obtained when operating under nominal conditions

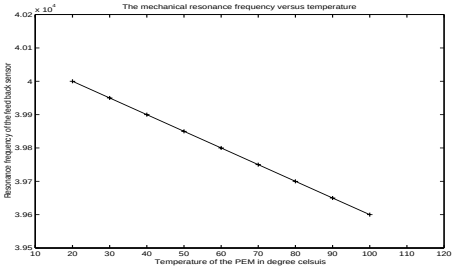

Figure 17: The mechanical resonance frequency versus the temperature of the rotary PEM

It must be emphasized that it is difficult to monitor the effect of temperature on the antiresonance frequency, but fortunately, only the mechanical resonance frequency is of crucial importance when the main target is the output performance in term of speed and position. Therefore it is only necessary to integrate in the model a tracking capability of the mechanical resonance frequency in order to maintain the output performance of the motor despite the temperature changes. Given the fact that the modal mass is a mechanical constant then the only parameters subject to variation under temperature changes are the damping and the stiffness/elasticity of the motional part whereas the changes

of the blocking admittance exist but are overlooked in the modeling process. The following relation represent the resonance behavior of the motional impedance as a function of temperature

$$\begin{cases} LC(2\pi f_r)^2 = 1 \\ LC_o(2\pi f_{r_o})^2 = 1 \\ f_r = f_{r_o} - \delta\,\Delta\theta \end{cases} \quad (42)$$

where f_{r_o} and f_r are resonance frequencies at the ambient and working temperature respectively, $\Delta\theta$ is the temperature gradient during operation and δ is the slop of the resonance-temperature characteristic. In term of equivalent circuit information the capacitance should be updated during the temperature changes in the following way

$$\begin{aligned} C &= \frac{1}{L(2\pi f_r)^2} = \frac{1}{L[2\pi(f_{r_o} - \delta\,\Delta\theta)]^2} \\ &= \frac{1}{L(2\pi f_{r_o})^2(1 - \frac{\delta}{f_{r_o}}\,\Delta\theta)^2} \approx C_o(1 + 2\frac{\delta}{f_{r_o}}\,\Delta\theta) \end{aligned}$$

where

$$\begin{cases} C_o = \frac{1}{L(2\pi f_{r_o})^2} \\ C = C_o(1 + 2\frac{\delta}{f_{r_o}}\,\Delta\theta) \end{cases} \quad (43)$$

for the USR60 $\delta = 5\ Hz.\deg^{-1}$ and $2\frac{\delta}{f_{r_o}} \approx 2.5e^{-4}$.

THE EFFECT OF VARYING TEMPERATURE IN A SIMULATED ENVIRONMENT

The mechanical resonance frequency of the motor shifts towards lower frequencies during the operation of the motor due to the temperature increase within the body of the stator. In order to overcome this problem in a simulated environment and therefore predict the performance of the motor despite the changes in its temperature a tracking facility which updates the temperature sensitive parameters is introduced in the equivalent circuit model. The figure 18 shows the prediction results achieved for the speed of the motor subject to temperature variation.

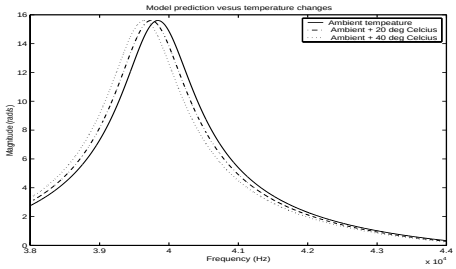

Figure 18: Speed prediction under varying temperature of the rotary PEM

From the figure 18 it can be noticed that the resonance frequency is a decreasing function of temperature and consequently for a fixed frequency above the resonance frequency the performance of the motor in terms of speed deteriorates. The main conclusion to be drawn is that for speed control purposes the influence of temperature changes must be integrated in model prediction for long term operations.

SIMULATION AND MODEL VALIDATION

The derived equivalent circuit model of the rotary PEM is implemented in Matlab-Simulink environment using the power-system toolbox. The results achieved by the simulated model are then compared to the measured characteristics in order to enhance the validity of the model.

THE EFFECT OF THE DRIVING FREQUENCY

The performance of the simulated model is given in terms of the output speed performance under varying frequency. The range of frequencies between 38 kHz and 44 kHz is explored and the achieved results are given in the figure 19

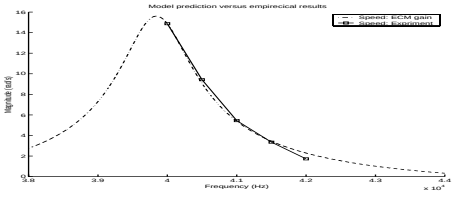

Figure 19: Comparison of speed-frequency characteristics for the unloaded rotary PEM: simulation and measurement

It must be emphasized that the results reported on this figure 19 are obtained for the free motor (i.e. no load) operating under its nominal conditions. On the same figure 19 are also reported the real speed measured directly on the motor. It can be noticed that there is agreement between the simulated model and the measured data which validates the equivalent circuit model of the free motor.

THE EFFECT OF VARYING TORQUE ON THE PEM

The figure 20 represent speed-frequency characteristics under different loading torques obtained from direct measurements when working under nominal conditions.

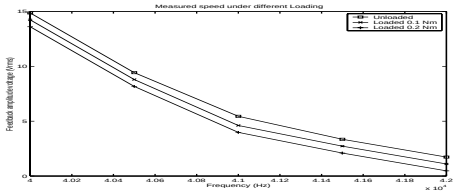

Figure 20: Speed-frequency characteristics of the rotary PEM under different loading torques: measurement

The range of torques between 0 Nm and 0.32 Nm is explored and the results achieved by the simulated model are given in the figure 21 for the torque loads 0.1 Nm and 0.2 Nm respectively.

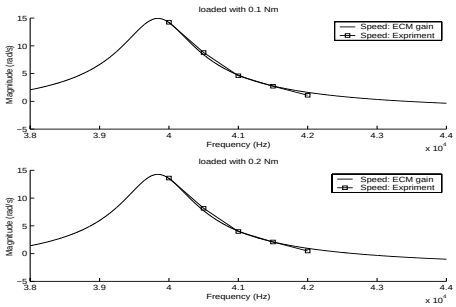

Figure 21: Comparison of speed-frequency characteristics for the rotary PEM subject to different loading torques: simulation and measurement

It can be noticed from the compared results that there is agreement between the simulated results and the measured results, which validates the model in the range of torques $[0\ Nm, 0.32\ Nm]$ and frequencies of interest i.e. in the neighborhood above the fundamental resonance frequency.

CONCLUSION

In this paper, an enhanced equivalent circuit model of a rotary traveling wave piezoelectric ultrasonic motor "shinsei type USR60" is derived. The modeling is performed on the basis of an empirical approach combined with the electrical network method and some simplification assumptions about the physical behavior of the real system. This paper highlights the importance of the electromechanical coupling factor, which is responsible for the electrical to mechanical energy conversion. The emphasis is put on the difference between the effective coupling factor and the modal coupling factor. The effective coupling factor is the force factor generated when only one excited dominating transverse mode of vibration is assumed and the modal coupling factor represents the direct contribution of each excited phase of the stator independently. The effect of the temperature on the mechanical resonance frequency is considered and thereby integrated in the final model for long term operations. The derived model has been simulated in a Matlab-Simulink environment by using the power-system toolbox. The achieved results have shown an agreement between the simulated results and the measured results, which validates the model in the range of torques $[0 - 0.32Nm]$ and frequencies of interest (i.e. in the neighborhood above the fundamental resonance frequency). Thereby the validity of the model has been established.

References

[1] T. Ikeda. *Fundamentals of Piezoelectricity*. Oxford University Press, 1996.

[2] W. Mason. *Physical Acoustics*. Harcourt Brace Jovanovich, Academic Press, 1964.

[3] Piecourt E. Nogarede, B. Modelisation of a travelling wave piezoelectric motor by equivalent electromechanical circuit. In *IECM'94*, 1994.

[4] Kenjo T. Sashida, T. *An Introduction to Ultrasonic Motors*. Oxford Science Publications, 1993.

Norddin Elghouti received the Master of Science in instrumentation in 1993 at Caen University in France and the MSEE in control engineering at Aalborg University in Danmark in 1997. Since then he is enrolled as a PhD student in the field of modeling and Control of electromechanial systems.

Jan Helbo received the MSEE in electrical and control engineering from Denmark Technical University in 1972. Currently he is an Associate Professor in the Department of Control Engineering at Aalborg University. His research interests have mainly been in the area of Robotics in the domain of real-time sensor-based manipulation and control. Recently his interests included modeling and control of Piezoelectric motors.